Revision 2

Priscillagrewite-(Y), $(Ca_2Y)Zr_2Al_3O_{12}$ - a new garnet of the bitikleite group from the Daba-Siwaqa area, the Hatrurim Complex, Jordan

Irina Galuskina[1]*, Evgeny Galuskin[1], Yevgeny Vapnik[2], Grzegorz Zeliński[3], Krystian Prusik[4]

[1]Institute of Earth Sciences, Faculty of Natural Sciences, University of Silesia, Będzińska 60, 41-200 Sosnowiec, Poland

[2]Department of Geological and Environmental Sciences, Ben-Gurion University of the Negev, P.O.B. 653, Beer-Sheva 84105, Israel

[3]Micro-Area Analysis Laboratory, Polish Geological Institute - National Research Institute, Rakowiecka 4, 00-975 Warsaw, Poland

[4]Institute of Materials Engineering, Faculty of Science and Technology, 75th Pułku Piechoty 1, 41-500 Chorzów, Poland

*e-mail: irina.galuskina@us.edu.pl

Word count: 6864

Abstract

Priscillagrewite-(Y), ideally $(Ca_2Y)Zr_2Al_3O_{12}$ (*Ia*-3*d*, a = 12.50 Å, V = 1953.13 Å^3, Z = 8), a new member of the garnet supergroup and bitikleite group, was discovered in a fluorapatite layer (metaphosphorite) hosted by varicolored spurrite marble in the Daba-Siwaqa area of the Transjordan plateau south of Amman, central Jordan. The Daba-Siwaqa area is the largest field of the Hatrurim Complex pyrometamorphic rocks distributed along the rift of the Dead Sea. Priscillagrewite-(Y) as well as other accessory minerals such as members of the brownmillerite-srebrodolskite series, fluormayenite, lakargiite, baghdadite, hematite,

sphalerite, zincite, garnet of the andradite-grossular series, tululite, vapnikite, minerals of the lime-monteponite series and members of the magnesiochromite-zincochromite series, cuprite, Y-bearing and Y-free perovskite are distributed irregularly in varicolored spurrite marble. The empirical formula of priscillagrewite-(Y), based on 12 oxygens, is $(Ca_{2.19}Y_{0.65}Ce^{3+}_{0.03}Nd^{3+}_{0.03}Gd^{3+}_{0.02}Dy^{3+}_{0.02}Er^{3+}_{0.02}Yb^{3+}_{0.02}La^{3+}_{0.01}Sm^{3+}_{0.01})_{\Sigma 3.00}(Zr_{1.79}Ti^{4+}_{0.13}Sb^{5+}_{0.07}U^{6+}_{0.01})_{\Sigma 2.00}(Al_{1.70}Fe^{3+}_{1.21}Si_{0.04}P^{5+}_{0.04})_{\Sigma 2.99}O_{12}$. A good match was obtained for electron backscatter diffraction (EBSD) patterns with a garnet model having a = 12.50 Å. The new garnet forms idiomorphic, isometric crystals up to 15 μm in size. It is transparent and has pale yellowish tinge, luster is vitreous. Priscillagrewite-(Y) is isotropic: n = 1.96 based on the Gladstone-Dale calculation using a = 12.50 Å and the empirical formula. The Mohs hardness is about 7-7.5. Density calculated from the empirical formula is 4.48 $g \cdot cm^{-3}$. Raman spectrum of priscillagrewite-(Y) is similar to the spectra of other minerals of the bitikleite group and contains the following bands (cm^{-1}): 150, 163, 240, 269, 289, 328, 496, 508, 726 and 785. The strongest lines of the calculated powder diffraction data are as follows [(*hkl*) d_{hkl} (*I*)]: (422) 2.552 (100), (642) 1.670 (96), (420) 2.795 (84), (400) 3.125 (72), (200) 4.419 (35), (640) 1.733 (32), (1042) 1.141 (25). Priscillagrewite-(Y) is interpreted to be a relic of the high-temperature association formed in the progressive stage of the peak pyrometamorphism conditions, when temperature could have reached close to 1000°C.

Key words: priscillagrewite-(Y), $(Ca_2Y)Zr_2Al_3O_{12}$, new mineral, garnet supergroup, bitikleite group, electron backscatter diffraction, Raman spectroscopy, Daba-Siwaqa, central Jordan

Introduction

Yttrium and the rare earth elements, particularly the heavy rare earth elements (HREE), are widespread in silicate garnet, and in rare cases reach a few percent. In addition, garnet

tends to concentrate these elements relative to associated rock-forming silicates (Kasowski and Hogarth 1968, Enami et al. 1995, Lanzirotti 1995, Bea 1996, Pyle and Spear 1999, Vaggelli et al. 2003, Katerinopoulou et al. 2009, Hönig et al. 2014, Gulbin 2016, Thakur et al. 2018). In the composition of this garnet Y and HREE prevail, which in general is characteristic for metamorphic and magmatic garnets. However, the garnet we report here, priscillagrewite-(Y), is only the second naturally occurring garnet to contain yttrium and rare earth elements in sufficient abundance to result in a distinct species, the first being menzerite-(Y), ideally $\{Y_2Ca\}[Mg_2](Si_3)O_{12}$ (Grew et al. 2010). Menzerite-(Y), with empirical formula $\{Y_{0.83}Gd_{0.01}Dy_{0.05}Ho_{0.02}Er_{0.07}Tm_{0.01}Yb_{0.06}Lu_{0.02}Ca_{1.37}Fe^{2+}_{0.49}Mn_{0.07}\}_{\sum 3}[Mg_{0.55}Fe^{2+}_{0.42}Fe^{3+}_{0.58}Al_{0.35}V_{0.01}Sc_{0.01}Ti_{0.08}]_{\sum 2}(Si_{2.82}Al_{0.18})_{\sum 3}O_{12}$ was found as relic cores in almandine from a felsic granulite in the Grenville Province at Bonnet Island, Ontario, Canada (Grew et al. 2010). High yttrium contents are also reported in garnets in ultrarefractory inclusions from carbonaceous chondrites: 0.57 Y *pfu* (*per formula unit*) in eringaite with the ideal formula $Ca_3Sc_2Si_3O_{12}$ from Vigarano CV3 meteorite (Ma 2012), and 0.83 Y *pfu* in the new garnet rubinite, $Ca_3Ti^{3+}_2Si_3O_{12}$, from the same meteorite (Ma et al. 2017).

Priscillagrewite-(Y), $(Ca_2Y)Zr_2Al_3O_{12}$ (*Ia*-3*d*, a = 12.50(3) Å, V = 1953.13(6) Å^3, Z = 8) was discovered in central Jordan in spurrite marble of the Daba-Siwaqa area belonging to the pyrometamorphic Hatrurim Complex. Pyrometamorphic rocks of the Hatrurim complex ("Mottled Zone") are distributed along the Dead Sea Transform Fault in Israel, Palestine and Jordan (Bentor et al. 1963; Gross 1977; Burg et al. 1991; Techer et al. 2006; Geller et al. 2012; Novikov et al. 2013, Khoury 2020).

Priscillagrewite-(Y) is assigned to the bitikleite group, whose total charge of cations at the tetrahedral site is 9, and which are generally hydroxyl-free, Si-free and Ca-rich (Grew et al. 2013). The general crystal chemical formula of the bitikleite group minerals previously described has also been characterized by valency-imposed double site occupancy at the *Y* site:

$\{X_3\}^{6+}[(Y,Y')_2]^{9+}(Z_3)^{9+}O_{12}^{24-}$. The minerals of the bitikleite group were found in altered xenoliths within ignimbrites of the Upper Chegem Caldera, Northern Caucasus, Russia and are represented by bitikleite, $Ca_3(Sb^{5+}Sn)Al_3O_{12}$, usturite, $Ca_3(Sb^{5+}Zr)Fe^{3+}{}_3O_{12}$, dzhuluite, $Ca_3(Sb^{5+}Sn)Fe^{3+}{}_3O_{12}$, and elbrusite, $Ca_3(Zr_{1.5}U^{6+}{}_{0.5})Fe^{3+}{}_3O_{12}$ (Galuskina et al. 2010a, b; Galuskina et al. 2013; Grew et al. 2013). Priscillagrewite-(Y) is the first garnet of the bitikleite group with valency-imposed double site-occupancy at the *X* site: $\{(X,X')_3\}^{7+}[Y_2]^{8+}(Z_3)^{9+}O_{12}^{24-}$.

The end member, $(Ca_2Y)Zr_2Al_3O_{12}$ doped with Ce^{3+}, an analogue of priscillagrewite-(Y), was first synthesized by Wang and Wang (2015), who reported space group *Ia*-3*d*, a = 12.4826(2) Å, V = 1945.00(3) Å^3 based on a Rietveld refinement of the crystal structure. The $(Ca_2Y)Zr_2Al_3O_{12}$:Ce^{3+} garnet was synthesized through a conventional solid-state method at 1400°C and atmospheric pressure (Wang and Wang 2015). Subsequent syntheses involved $(Ca_2Y)Zr_2Al_3O_{12}$ doped with Eu^{3+} and other rare earth elements (e.g., Wang et al. 2016; Qu et al. 2020) and Ce^{3+}-doped compositions in the $(Ca_{2-x}Y_{1+x})Zr_{2-x}Al_{3+x}O_{12}$ series, where $0 \leq x \leq 0.6$ (Wang et al. 2017). These doped garnets can be used as a light-emitting diode material.

The mineral and name (IMA2020–002) were approved by the Commission on New Minerals, Nomenclature and Classification of the International Mineralogical Association. The name is in honor of Priscilla Croswell Perkins Grew, born in Glens Falls, New York, USA on October 26, 1940. She is Professor Emerita in the Department of Earth and Atmospheric Sciences, University of Nebraska-Lincoln, and is Director Emerita of the State Museum of Natural History at the University of Nebraska. Since 1998, she has coordinated the federal repatriation of human remains and archeological objects from the University of Nebraska-Lincoln to Native American Tribes. She is a Fellow of the Mineralogical Society of America, and in 1999 was awarded the American Geosciences Institute Medal in Memory of Ian Campbell for Superlative Service to the Geosciences. Her early research was on

metamorphic petrology of blueschists and eclogites in California. As Priscilla P. Dudley, she published the first electron beam scanning photographs of oscillatory zoning in eclogitic garnet (Dudley, 1969).

The holotype material has been deposited in the mineralogical collection of Fersman Mineralogical Museum, Leninskiy Prospekt, 18/k, 115162 Moscow, Russia, catalogue number 5540/1.

In the present article we provide the results of our investigation of the morphology, composition and mineral assemblage of priscillagrewite-(Y). Electron microprobe analyses, Raman spectroscopy and electron backscatter diffraction (EBSD) yielded the data essential for recognizing priscillagrewite-(Y) as a new mineral species.

Analytical methods

The small size of the priscillagrewite-(Y) crystals dictated the methodology deployed for investigation. Identification, morphology and semi-quantitative composition of garnet and associated minerals, as well as selection of garnet grains for further investigation, were performed using a Phenom XL table top scanning electron microscope with CeB_6 cathode (Institute of Earth Sciences, Faculty of Natural Sciences, University of Silesia, Poland). The chemical composition of priscillagrewite-(Y) was measured with a Cameca SX100 electron microprobe analyzer (Micro-Area Analysis Laboratory, Polish Geological Institute - National Research Institute, Warsaw, Poland): WDS, accelerating voltage= 15 kV, beam current = 40 nA, beam diameter ~ 1 μm. REE were measured using LLIF crystal during 30 s at peak and 15 s in background, Y was measured using LPET crystal during 40 s and 20 s at background. The following standards and lines were used, the detection limit is given in wt.% in brackets: P&H U-glass synthetic – U*M*β (0.04); MAC Sb metal – Sb*L*α (0.03); SPI apatite – Ca*K*α (0.01), P*K*α (0.01); SPI ZrO_2 – Zr*L*α (0.03), Hf*L*α (0.08); SPI rutile – Ti*K*α (0.04); SPI

This is the peer-reviewed, final accepted version for American Mineralogist, published by the Mineralogical Society of America.
The published version is subject to change. Cite as Authors (Year) Title. American Mineralogist, in press.
DOI: https://doi.org/10.2138/am-2021-7692. http://www.minsocam.org/

sanidine – Si*K*α (0.01), Al*K*α (0.01); SPI olivine – Fe*K*α (0.05); YPO_4 synthetic – Y*K*α (0.04); $LaPO_4$ synthetic – La*L*α (0.10); $CePO_4$ synthetic – Ce*L*α (0.10); $NdPO_4$ synthetic – Nd*L*β (0.15); SmPO4 synthetic – Sm*L*β (0.17); $GdPO_4$ synthetic – Gd*L*α (0.08); $DyPO_4$ synthetic – Dy*L*α (0.09); $ErPO_4$ synthetic – Er*L*α (0.10); $YbPO_4$ synthetic – Yb*L*α (0.11).

The symmetry and cell parameters of priscillagrewite-(Y) were determined by electron backscatter diffraction (EBSD) using a high-performance scanning electron microscope JSM-6480 equipped with EBSD (Faculty of Science and Technology, University of Silesia, Poland). The microprobe thin section, in which the garnet composition measurements were performed, was re-polished using Al_2O_3 suspension of 20 nm particle size. The EBSD images were recorded with a HKL Nordlys II camera using a 30 kV beam energy. The geometry calibration of the SEM and EBSD system was carried out on Si for two detector distances, i.e. 177 mm (normal working position) and 150 mm (camera refracted position). The program Channel5 (Day and Trimby, 2004) was used for the interpretation of the EBSD diffraction patterns. An optimization procedure was applied to estimate the symmetry and cell parameter of priscillagrewite-(Y). First, an approximate cell parameter was calculated on the basis of the empirical formula for priscillagrewite-(Y) (Table 1) according to the equation (Strocka et al. 1978): a = b1+b2rX+b3rY+b5rXrY+ b6rXrZ+ b4rZ (Å), where b1 = 7.02954; b2 = 3.31277; b3 = 2.49398; b4 = 3.34124; b5 = –0.87758; b6 = –1.38777 and rX, rY, rZ = weight-averaged effective ionic radii of cations (Shannon 1976). A structure file was created using Hawthorne's (1981) recommendations for calculating the oxygen positions in the garnet structure and the Crystal Maker program with the *a* parameter = 12.50 Å (Table S1, deposit item). Lastly, fitting the EBSD patterns with the structure file gave MAD ≈ 0.5, which indicates a good agreement.

Powder X-ray diffraction (PXRD) data were not obtained because it was not possible to obtain a sufficient amount of pure material of priscillagrewite-(Y). The powder pattern was

calculated based on the single-crystal theoretical model (Table S2, deposit item) using PowderCell 2.4 software (Kraus and Nolze 1996).

The Raman spectra of priscillagrewite-(Y) recorded on a WITec alpha 300R Confocal Raman Microscope (Institute of Earth Science, Faculty of Natural Sciences, University of Silesia, Poland) equipped with an air-cooled solid laser 488 nm and a CCD camera operating at -61°C. The laser radiation was coupled to a microscope through a single-mode optical fibre with a diameter of 3.5 μm. An air Zeiss (LD EC Epiplan-Neofluan DIC–100/0.75NA) objective was used. Raman scattered light was focused by an effective pinhole size of about 30 μm and a monochromator with a 600 mm^{-1} grating. The power of the laser at the sample position was 30 mW. An integration times of 5 s with an accumulation of 20 scans, and a resolution of 3 cm^{-1} was chosen. The monochromator was calibrated using the Raman scattering line of a silicon plate (520.7 cm^{-1}). Baseline correction was performed using the Spectracalc software package GRAMS (Galactic Industries Corporation, NH, USA). Band fitting was performed using a Gauss-Lorentz cross-product function, with the minimum number of component bands used for the fitting process.

Results

Occurrence

Priscillagrewite-(Y) was found in a single fine-grained green fluorapatite layer about 6 cm in thickness (metaphosphorite) in spurrite-bearing marble in a quarry (N 31°32′31″, E 36°10′19″) in the Tulul Al Hammam area, which is in the pyrometamorphic field of the Daba-Siwaqa area, central Jordan. The priscillagrewite-(Y) crystals with rounded inclusions of fluorapatite (Fig. 1) are confined to a single micro-layer about 1 cm in thickness.

The varicolored marble belongs to the upper part of the Maastrichtian-Paleogene Muwaqqar Chalk-Marl Unit (Khoury et al. 2015, Sokol et al. 2017, Khoury 2020). This unit

was converted into varicolored marble by pyrometamorphism, and is thus included in the Hatrurim Complex (Mottled Zone of Picard 1931). The pyrometamorphosed units, which are represented by gehlenite-, larnite- and spurrite-bearing rocks, are widespread along the rift of the Dead Sea in the territory of Israel, Palestine and Jordan (Picard 1931, Bentor et al. 1963, Gross 1977, Kolodny 1979, Burg et al. 1999, Geller et al., 2012, Novikov et al., 2013, Khoury et al. 2014). The Daba-Siwaqa area embraces numerous outcrops of the Hatrurim Complex rocks located at the Transjordan plateau south of Amman (Novikov et al., 2013, Khoury et al. 2015, Khoury 2020).

In the sample with priscillagrewite-(Y) the following minerals were detected in addition to spurrite and fluorapatite: minerals of the brownmillerite-srebrodolskite series, fluormayenite, lakargiite, baghdadite, hematite, sphalerite, zincite, garnet of the andradite-grossular series, tululite, vapnikite, minerals of the lime-monteponite series, members of the magnesiochromite-zincochromite series, cuprite, Y-bearing and Y-free perovskite, ellinaite, and mcconnellite.

Physical and optical properties

Priscillagrewite-(Y) forms idiomorphic crystals up to 15 μm in size. Typical cross-sections indicate that the faces of the rhombic dodecahedron and deltoid dodecahedron (forms {110} and {211}) are observed (Figs. 1C-F). The crystals are transparent and have a pale yellowish tinge (Fig. 1C) and vitreous luster. They are characterized by absence of cleavage and have conchoidal fracture. Priscillagrewite-(Y) is isotropic, n = 1.96 based on Gladstone-Dale calculation using a = 12.50 Å and the empirical formula (see below). Because of the limited number of priscillagrewite-(Y) grains available for measuring hardness, we were able to obtain only an imperfect indention on one grain using the microindentation tester at 10 g. The microhardness is estimated to lie in the range VHN_{10} =1080-1240 kg/mm^2, equivalent to a Mohs hardness of about 7-7.5. The calculated density based on the empirical formula and unit

cell volume is equal 4.48 g·cm^{-3}. Unfortunately, because of small size of priscillagrewite-(Y) crystals, other physical properties could not be determined.

Chemical composition

The mean chemical composition of priscillagrewite-(Y) is presented in Table 1. Sum of rare earth elements and yttrium is 15.35 wt.%, which gives 0.81 apfu when calculated for the garnet stoichiometry. LREE and HREE contents are about equal, both total ~0.08 apfu.

The empirical priscillagrewite-(Y) formula calculated on the basis of 12 O is $(Ca_{2.19}Y_{0.65}Ce^{3+}_{0.03}Nd^{3+}_{0.03}Gd^{3+}_{0.02}Dy^{3+}_{0.02}Er^{3+}_{0.02}Yb^{3+}_{0.02}La^{3+}_{0.01}Sm^{3+}_{0.01})_{\Sigma 3.00}(Zr_{1.79}Ti^{4+}_{0.13}Sb^{5+}_{0.07}U^{6+}_{0.01})_{\Sigma 2.00}(Al_{1.70}Fe^{3+}_{1.21}Si_{0.04}P^{5+}_{0.04})_{\Sigma 2.99}O_{12}$, which can be simplified to the formula $\{Ca_{2.19}(Y,REE)_{0.81}\}_{\Sigma 3.00}[(Zr,Ti)_{1.92}Sb^{5+}_{0.07}U^{6+}_{0.01}]_{\Sigma 2.00}([Al,Fe]_{2.91}Si_{0.04}P^{5+}_{0.04}]_{\Sigma 2.99}O_{12}$. The end-member formula of priscillagrewite-(Y) is $\{Ca_2Y\}[Zr_2](Al_3)O_{12}$, taking into consideration the dominant-valency rule and valency-imposed double site-occupancy (Hatert and Burke 2008). As Y is dominant among the rare earth and related elements, the Levinson modifier is Y.

It is likely that the phosphorus detected in priscillagrewite-(Y) is caused by the presence of fluorapatite, which is in intimate intergrowth with it. Also in the Raman spectrum a weak band from fluorapatite is observed, although measurements were performed in the confocal regime (Fig. 2).

Raman spectroscopy

Raman spectrum of priscillagrewite-(Y) is similar to the spectra of other minerals of the bitikleite group (Galuskina et al. 2010a). The following main bands were observed in the Raman spectrum of priscillagrewite-(Y), which are related to the defined types of vibrations (Fig. 2, cm^{-1}): *Translation*(X) – 150 $T(Ca^{2+})$ and 163 $T(Y^{3+})$; *Translation*(ZO_4) - 240 $T(FeO_4)^{5+}$ and 269 $T(AlO_4)^{5+}$, *Rotation*($ZO)_4$ – 289 $R(FeO_4)^{5+}$ and 328 $R(AlO_4)^{5+}$, *bending*(Z-

O) – 496 (Fe^{3+}-O)$_{bend}$ and 508 (Al-O)$_{bend}$, *streching* (Z-O) – 726 (Fe^{3+}-O)$_{str}$ and 785 (Al-O)$_{str}$ (Schingaro et al. 2001, Galuskina et al. 2010a, 2013, Monteseguro et al. 2014, Uher et al. 2015, Kostić et al. 2015).

Crystallography (electron backscatter diffraction)

The crystal structure of priscillagrewite-(Y) could only be determined by using EBSD because of small size of the crystals, abundant inclusions and rarity. EBSD does not provide precision structural data, but allows comparison of a structure with a model, by which one can determine the space group and estimate unit cell parameters. In the case of cubic garnet a theoretical calculation is possible if the unit cell parameter *a* can be specified, which has been done for priscillagrewite-(Y) (Table S1, deposit item). The EBSD patterns for priscillagrewite-(Y) were obtained at working distances of 150 mm and 177 mm. Fitting of the EBSD data (WD 177 mm, model structure of garnet with a = 12.50 Å, Table S1, deposit item) of crystals shown in Fig. 1C, D resulted in good fitting parameters MAD = 0.53 and 0.52, respectively (Fig. 3). In summary, priscillagrewite-(Y) has the garnet structure, space group *Ia*-3*d* with a = 12.50 Å (Fig. 4).

Discussion

Classification

There are 17 chemical elements present in priscillagrewite-(Y) in amounts exceeding the detection limit of the electron microprobe, most notably, the Y content reaches 11.7 wt.% Y_2O_3 and REE, 4.7 wt.% REE_2O_3, with roughly equal contents of heavy and light REE. The calculation of end-members that is often used for minerals of the garnet supergroup (e.g., Grew et al. 2013) should not be applied to such complex compositions. For example, if we begin calculation from the priscillagrewite-(Y) end-member, $YCa_2Zr_2Al_3O_{12}$, then this end

member's proportion will be 56.7%, which is determined by the amount of Al at the tetrahedral *Z* site. But if we begin the calculation from the end-member $YCa_2Zr_2Fe^{3+}{}_3O_{12}$, then the proportion of $YCa_2Zr_2Fe^{3+}{}_3O_{12}$ will be ~40%, and the priscillagrewite-(Y) end-member will be only ~25%. Therefore, to define the ideal end-member formula of priscillagrewite-(Y), $YCa_2Zr_2Al_3O_{12}$, the dominant valency rule is applied (Hatert and Burke 2008).

In the *Y*-site classification diagram priscillagrewite-(Y) plots in the field of schorlomite group minerals (Fig. 5A), whereas in the *Z*-site diagram the field of priscillagrewite-(Y) plots with bitikleite outside the field of the schorlomite group minerals (Fig. 5B). Since group designation depends first of all on occupancy at the *Z* site (Grew et al. 2013), priscillagrewite-(Y) is included in the bitikleite group. The relatively high proportion of Fe^{3+} at the *Z*-site in priscillagrewite-(Y) (Table 1) implies that the Fe^{3+}-analog of priscillagrewite-(Y) corresponding to the end-member formula $(Ca_2Y)Zr_2Fe^{3+}{}_3O_{12}$ could be found in Nature; it has been synthesized (Geller et al. 1960).

Priscillagrewite-(Y) has +8 charge at the *Y* site and thus differs from other minerals of the bitikleite group, which have +9 charge at the *Y* site. The charge deficiency is balanced by Y^{3+} replacing one Ca^{2+} at the *X* site. Thus, there are two isomorphic substitution schemes relating priscillagrewite-(Y) to other minerals of the bitikleite group: $\{^{X}Ca^{2+} + {}^{Y}Sb^{5+}\}^{7+}$ (bitikleite, usturite, dzhuluite) $\rightarrow$ $\{^{X}Y^{3+} + {}^{Y}Zr^{4+}\}^{7+}$ and $\{^{X}Ca^{2+} + {}^{Y}(U^{6+}{}_{0.5}+R^{4+}{}_{0.5})\}^{7+}$(elbrusite) $\rightarrow$ $\{^{X}Y^{3+} + {}^{Y}Zr^{4+}\}^{7+}$ (Fig. 5A, 6).

The binary diagram for occupancy of the *X* site, 3Ca pfu – 3(Y+REE) pfu (Fig. 6), shows the relationship between the compositional range of priscillagrewite-(Y) and the compositions of minerals in the bitikleite and schorlomite groups, as well the synthetic yttrium garnets $Y_3Al_2Al_3O_{12}$ (YAG) and $Y_3Fe^{3+}{}_2Fe^{3+}{}_3O_{12}$ (YIG), in terms of constituents at the *X* site. We did not consider solid-solutions between priscillagrewite-(Y) and other garnet species because in

this case the isomorphic substitutions take place at all three cation sites, rather than at the two sites relating priscillagrewite-(Y) with members of the bitikleite and schorlomite groups, and with YAG and YIG (Fig. 6). Valency-imposed double-site occupancy at the all three sites can result in improbable intermediate boundary compositions in terms of the end-members, for example, the intermediate $\{Ca_{1.5}Y_{1.5}\}(ZrMg)[Si_{1.5}Al_{1.5}]O_{12}$ composition between priscillagrewite-(Y) and menzerite-(Y), $\{Y_2Ca\}[Mg_2](Si_3)O_{12}$, is equivalent to the sum of $½\{Ca_2Y\}(Zr_2)[Al_3]O_{12}$ + $½\{Y_2Ca\}(Mg_2)(Si_3)O_{12}$ or the sum $½\{Y_3\}(ZrMg)[Al_3]O_{12}$ + $½\{Ca_3\}(ZrMg)[Si_3]O_{12}$.

Origin and conditions of formation

Varicolored marbles with apatite layers of different thickness (~1 mm to 0.5 m) containing priscillagrewite-(Y) and other unusual minerals are the products of pyrometamorphism of the upper part of the Muwaggar formation in central Jordan represented by bituminous marls and limestone containing phosphorite intercalations (Khoury et al. 2016, Khoury 2020). The Muwaggar formation is underlain by phosphorites of the Amman formation (Abed et al. 2016, Khoury 2020). Apatite enrichment of certain layers in bituminous marls and limestones of the Muwaggar formation could be the result of erosion and re-deposition of earlier formed phosphorites of the Amman formation, a process accompanied by concentration in some thin rock layers with detrital minerals such as zircon, monazite and xenotime, which became a source of Zr, Y and REE for priscillagrewite-(Y). Although rocks containing abundant fluorapatite might have higher concentrations of REE than other rocks, e.g., Abed and Abu Murry (1997) reported that total REE concentrations (200-300 ppm) from upper Cretaceous phosphorites in central Jordan average over twice that of shale, we consider it unlikely that the Y and REE in priscillagrewite- (Y) originated in fluorapatite. Although fluorapatite can incorporate Y and REE, it does not incorporate

significant Zr; the only plausible source of Zr for priscillagrewite-(Y) is thus detrital zircon. We conclude that detrital phases were most likely also the source of Y and REE.

In similar varicolored marble from the Tulul Al Hammam area the new mineral tululite, $Ca_{14}(Fe^{3+},Al)(Al,Zn,Fe^{3+},Si,P,Mn,Mg)_{15}O_{36}$ was found (Khoury et al. 2016), which is also associated with priscillagrewite-(Y). Khoury et al. (2016) estimated 800-850 °C for formation of tululite-bearing rock. In making this estimate, Khoury et al. (2016) assumed that partial decarbonatization of the carbonate protolith led to the calcite-fluorellestadite-spurrite-brownmillerite association, but without larnite and hatrurite, which would have required yet higher temperatures. The absence of larnite in pyrometamorphic rocks of Jordan is the main difference compared to the pyrometamorphic rocks of Israel and Palestine, in which larnite and flamite are rock-forming minerals (Gfeller et al. 2015, Sokol et al. 2015, 2019). Nevertheless, it must be emphasized that in the pyrometamorphic rocks of central Jordan we have found small larnite relics in apatite-spurrite varicolored marbles as well as thin layers of larnite pseudoconglomerates in grey spurrite-bearing rocks. The higher temperature pyrometamorphic rocks in the Daba-Siwaqa field are exposed to the south of the type-locality of priscillagrewite-(Y). These rocks are known for Fe and Ni phosphides discovered in pyroxene-bearing paralava formed over a wide temperature range, 850 to 1370°C (Britvin et al. 2017). Consequently, it cannot be excluded that the varicolored marbles in the Tulul Al Hammam area are the product of regressive secondary carbonatization of the primary high-temperature pyrometamorphic rocks, which can contain high-temperature Ca-silicates and CaO (lime).

In the sample of varicolored marble priscillagrewite-(Y) is associated with lakargiite, $CaZrO_3$, perovskite, $CaTiO_3$, a Y-bearing perovskite, $(Ca,Y)(Ti,Fe)O_3$ (about 10% of $YFeO_3$), ellinaite, β-$CaCr_2O_4$, mcconnellite, $CuCrO_2$, and spinel of the magnesiochromite-zincochromite series $(Mg,Zn)Cr_2O_4$. It can be assumed that these accessory oxide minerals are

relics of the high-temperature association of pyrometamorphic rocks of the progressive stage. Zirconium-bearing perovskite – lakargiite, $CaZrO_3$, containing uranium and commonly forming fine-grained pseudomorphs after detrital zircon, is one of the characteristic accessory minerals of pyrometamorphic rocks of the Hatrurim Complex (Galuskin et al. 2013, Khoury et al. 2015, 2016, Khoury 2020, Sokol et al. 2016). Crystallization of $CaZrO_3$ in the system ZrO_2-$CaCl_2$-Na_2CO_3 begins at 700°C in the presence of a liquid phase under laboratory conditions (Li et al. 2007). Synthesis of $CaZrO_3$ in the absence of a liquid phase occurs only above 1100°C (Yeo et al. 2004; Park 2007). The pyrometamorphic processes caused by organic-fuel combustion takes place at high temperature and low pressure, with fluids playing an insignificant role and solid-state transformation of the protolith being largely isochemical (Grapes 2010). Pyrometamorphic rocks inherit protolith geochemical heterogeneity to a great extent as a result of such transformations. Priscillagrewite-(Y) and associated accessory minerals containing Cr, Ti, Zr formed as a result of the reactions of detrital minerals (e.g., zircon, chromite, xenotime, monazite) with simple oxides (and rarer sulfides) of Ca, Mg, Zn and Cu. As noted above, accessory lakargiite and, appropriately, priscillagrewite-(Y) can crystallize at a temperature higher than temperature of varicolored marble crystallization. Ellinaite, β-$CaCr_2O_4$, which is associated with priscillagrewite-(Y), is also found in paralava of the Hatrurim Complex in the Negev Desert, Israel, where it formed at temperatures estimated to range 1000-1300°C (Sharygin et al. 2019). It is likely that the formation temperature of some of the accessory minerals was higher than the temperature of calcite-fluorapatite-spurrite assemblage of the varicolored marbles of the Daba-Siwaqa area. This temperature might be 100-150°C higher than the temperature of the main varicolored marble mineral assemblage, i.e. about 1000°C. Combustion involves non-equilibrium processes and can be expected to be of short duration or with local increases in temperature, for example, within cracks and fissures. Such temperature fluctuations might not be evident in the most

widespread assemblages, but would appear only in very restricted occurrences of accessory mineral indicators of the peak temperature of pyrometamorphism.

Implications

In 2010 a new garnet - eringaite, $Ca_3Sc_2Si_3O_{12}$, was discovered in a giant xenolith of skarn within trap rock exposed on the banks of the Wiluy River, Sakha Republic – Yakutia (Galuskina et al. 2010c). In 2012 eringaite was detected in the Vigarano V3 chondrite and later in other chondrites (Ma 2012, Krot et al. 2019). Ma (2012) considered eringaite as an ultrarefractory silicate - likely the first garnet formed in the solar system. Eringaite from meteorites is characterized by a Y content up to 0.57 pfu, which Ma et al. (2012) and Krot et al. (2019) inferred to occupy the octahedral *Y* site. However, it is more likely that Y occupies the *X* site as it does in menzerite-(Y) (Grew et al. 2010), priscillagrewite-(Y), and in other silicate garnets in which it is present as a minor constituent (Carlson et al. 2012, 2014). In 2017 a new garnet rubinite, $Ca_3Ti^{3+}{}_2Si_3O_{12}$, in which the Y content varies from 0 to 0.83 apfu, was found in the V3 Vigarano, Allende, and Efremovka chondrites. Rubinite is also interpreted to have formed among the first solid materials in the solar nebula (Ma et al. 2017). In the solar nebula, eringaite and rubinite formed under highly reducing conditions, such that trivalent Ti is present, either as a minor constituent (eringaite) or as an essential component (rubinite) (Ma 2012, Ma et al. 2017). As Zr-, Sc- and Y-rich minerals are often identified in ultrarefractory calcium-aluminum-rich inclusions in chondrites (Krot et al. 2019), we suggest that there is a reasonable chance of finding the Y-Zr mineral priscillagrewite-(Y) in such inclusions, i.e., priscillagrewite-(Y) containing minor Ti^{3+} and Sc, but no Fe^{3+}, is a candidate for the third garnet species originating in the solar nebula. Indeed, the rubinite from Vigarano has a composition $(Ca_{1.89}Y_{0.83}Mg_{0.28})(Ti^{3+}{}_{0.59}Sc_{0.50}Zr_{0.72}Mg_{0.2}V_{0.02}Cr_{0.01})(Si_{1.64}Al_{1.18}Ti^{4+}{}_{0.07}Fe_{0.06})O_{12}$ (Ma et al.

2017), remarkably close to priscillagrewite-(Y), differing by predominance of trivalent cations over quadrivalent cations at the Y site and a predominance of quadrivalent cations over trivalent cations at the Z site.

The green fluorapatite-bearing metaphosphorite layer (Fig. 1A) hosting priscillagrewite-(Y) is also of potential relevance to Near Eastern archaeology. Certain green stone beads found at important Neolithic archeological sites are reported as being composed of "Dabba Marble" (Wright et al. 2008; Bar-Yosef Mayer and Porat 2008). Archeologists use the term "Dabba Marble" for artifacts composed of colorful pyrometamorphic calcareous rocks derived from the Mottled Zone in the upper part of the Muwaqqar Chalk-Marl Unit (Wright et al., 2008). Early peoples were attracted to the green color of fluorapatite-rich metaphosphorite similar to the rock hosting priscillagrewite-(Y). The first use of stone to make green beads and pendants is considered by Bar-Yosef Mayer and Porat (2008) to be associated with the onset of agriculture in the Near East. Thus, furthering our understanding of the geological origin of the green phosphatic rocks from Daba Marble Quarry is relevant to research in archaeology.

Acknowledgements. We thank reviewers Andrew Locock and Thomas Armbruster for their valuable comments and suggestions. Investigations were partially supported by the National Science Centre of Poland Grant no. 2016/23/B/ST10/00869.

References

Abed, A.M. and Abu Murry, O.S (1997) Rare Earth element geochemistry of the Jordanian Upper Cretaceous Phosphorites. Arab Gulf Journal of Scientific Research, 15(1), 41-61.

Abed, A., Jaber, O., Alkuisi, M., and Sadaqah, R. (2016) Rare earth elements and uranium geochemistry in the Al-Kora phosphorite province, late cretaceous, northwestern Jordan. Arabian Journal of Geosciences, 9,187. https://doi.org/10.1007/s12517-015-2135-6.

Bar-Yosef Mayer, D. and Porat, N. (2008) Green stone beads at the dawn of agriculture. Proceedings of the National Academy of Sciences, 105 (25), 8548-8551.

Bea, F. (1996) Residence of REE, Y, Th and U in granites and crustal protoliths; implications for the chemistry of crustal melts. Journal of Petrology, 37(3), 521-552.

Bentor, Y.K., Gross, S., and Heller, L. (1963) Some unusual minerals from the "Mottled Zone" complex, Israel. American Mineralogist, 48, 924-930.

Britvin, S.N., Murashko, M.N., Vapnik, E., Polekhovsky, Y.S., and Krivovichev, S.V. (2017) Barringerite Fe_2P from Pyrometamorphic Rocks of the Hatrurim Formation, Israel. Geology of Ore Deposits, 59(7), 619-625.

Burg, A., Kolodny, Y., and Lyakhovsky, V. (1999) Hatrurim-2000: the "Mottled Zone" revisited, forty years later. Israel Journal of Earth Sciences, 48, 209-223.

Burg, A., Starinsky, A., Bartov, Y., and Kolodny, Y. (1991) Geology of the Hatrurim Formation ("Mottled Zone") in the Hatrurim basin. Israel Journal of Earth Sciences. 40, 107-124.

Carlson, W.D. (2012) Rates and mechanism of Y, REE, and Cr diffusion in garnet. American Mineralogist, 97, 1598–1618.

Carlson, W.D., Gale, J.D., and Wright, K. (2014) Incorporation of Y and REEs in aluminosilicate garnet: Energetics from atomistic simulation. American Mineralogist, 99, 1022–1034.

Day, A. and Trimby, P. (2004) Channel 5 Manual HKL Technology Inc., Hobro, Denmark.

Dudley, P. (1969) Electron microprobe analyses of garnet in glaucophane schists and associated eclogites. American Mineralogist, 54, 1139-1150.

Enami, M., Cong, B., Yoshida, T., and Kawabe, I. (1995) A mechanism for Na incorporation in garnet: An example from garnet in orthogneiss from the Su-Lu terrane, eastern China. Am. Mineral. 80, 475-482.

Galuskin, E.V., Kusz, J., Armbruster, T., Galuskina, I.O., Marzec, K., Vapnik, Ye., and Murashko, M. (2013) Vorlanite, $(CaU^{6+})O_4$, from Jabel Harmun, Palestinian Autonomy, Israel. American Mineralogist, 98 (11-12): 1938–1942.

Galuskina, I.O., Galuskin, E.V., Armbruster, T., Lazić, B., Dzierżanowski, P., Gazeev, V.M, Prusik, K., Pertsev, N.N., Winiarski, A., Zadov, A.E., Wrzalik, R., and Gurbanov, A.G. (2010a) Bitikleite-(SnAl) and bitikleite-(ZrFe): New garnets from xenoliths of the Upper Chegem volcanic structure, Kabardino-Balkaria, Northern Caucasus, Russia. American Mineralogist, 95(7), 959-967.

Galuskina, I., Galuskin, E.V., Armbruster, T., Lazic, B., Kusz, J., Dzierżanowski, P., Gazeev, V., Pertsev, N., Prusik, K., Zadov, A., Winiarski, A., Wrzalik, R., and Gurbanov, A. (2010b) Elbrusite-(Zr) - a new uranian garnet from the Upper Chegem caldera, Kabardino-Balkaria, Northern Caucasus, Russia. American Mineralogist, 95, 1172-1181.

Galuskina, I.O., Galuskin, E.V., Kusz, J., Dzierżanowski, P.,Prusik, K., Gazeev, V.M., Pertsev, N.N., and Dubrovinsky, L. (2013) Dzhuluite, $Ca_3SbSnFe^{3+}{}_3O_{12}$, a new bitikleite-group garnet from the Upper Chegem Caldera, Northern Caucasus, Kabardino-Balkaria, Russia. European Journal of Mineralogy, 25, 231-239.

Galuskina, I.O., Galuskin, E.V., Lazic, B., Armbruster, T., Dzierżanowski, P., Prusik, K., and Wrzalik, R. (2010c) Eringaite, $Ca_3Sc_2(SiO_4)_3$, a new mineral of the garnet group. Mineralogical Magazine, 74, 365-373.

Galuskina, I.O., Krüger, B., Galuskin, E.V., Vapnik, Y., and Murashko, M. (2019) Khurayyimite, IMA 2018-140. CNMNC Newsletter No. 48, April 2019, page 316; Mineralogical Magazine, 83, 315–317.

Geller, S., Bozorth, R. M., Miller, C. E., and Davis, D. D. (1960) Crystal chemical and magnetic studies of garnet systems $\{YCa_2\}[M^{4+}_2](Fe_3)O_{12}$ -$\{Y_3\}[Fe_2](Fe_3)O_{12}$, M = Zr or Hf. Journal of Physics and Chemistry of Solids, 13, 28-32.

Geller Y.I., Burg A., Halicz L., and Kolodny Y. (2012) System closure during the combustion metamorphic "Mottled Zone" event, Israel. Chemical Geology, 334, 25-36.

Gfeller, F., Widmer, R., Krüger, B., Galuskin, E. V., Galuskina, I. O., and Armbruster, T. (2015). The crystal structure of flamite and its relation to Ca_2SiO_4 polymorphs and nagelschmidtite. European Journal of Mineralogy, 27(6), 755-769.

Grapes, R. (2010) Pyrometamorphism, 2nd ed. Springer-Verlag, Berlin Heidelberg, 365 pp.

Grew, E.S., Marsh, J.H., Yates, M.G., Lazic, B., Armbruster, T., Locock, A., Bell, S.W., Dyar, M.D., Bernhardt, H.J., and Medenbach O. (2010) Menzerite-(Y), a new species, $\{(Y,REE)(Ca,Fe^{2+})_2\}[(Mg,Fe^{2+})(Fe^{3+},Al)](Si_3)O_{12}$, from a felsic granulite, Parry Sound, Ontario, and a new garnet end-member, $\{Y_2Ca\}[Mg_2](Si_3)O_{12}$. The Canadian Mineralogist, 48, 1171-1193.

Grew, E. S., Locock, A.J, Mills, S.J., Galuskina, I.O., Galuskin, E.V., and Hålenius U. (2013) Nomenclature of the garnet supergroup. American Mineralogist, 98(4), 785-811.

Gross, S. (1977) The mineralogy of the Hatrurim Formation, Israel. Geological Survey of Israel Bulletin, 70, 80p.

Gulbin, Yu. L. (2016) Zonal REE + Y profiles in garnet and their genetic implications: a case study of metapelites from the Northern Ladoga region. Geology of Ore Deposits, Vol. 58, No. 7, pp. 559–567.

Hatert, F. and Burke, E.A.J. (2008) The IMA-CNMNC dominant-constituent rule revised and extended. The Canadian Mineralogist, vol. 46, 717-728.

Hawthorne, F.C. (1981) Some systematics of the garnet structure. Journal of Solid State Chemistry, 37(2), pp.157-164.

Hönig, S., Čopjaková, R., Škoda, R., Novák, M., Dolejš, D., Leichmann, and J., Vašinová Galiová M. (2014) Garnet as a major carrier of the Y and REE in the granitic rocks: An example from the layered anorogenic granite in the Brno Batholith, Czech Republic. American Mineralogist, 99, 1922–1941.

Kasowski, M.A. and Hogarth, D.D. (1968) Yttrian andradite from the Gatineau Park, Quebec. The Canadian Mineralogist, 9, 552-558.

Katerinopoulou, A., Katerinopoulos, A., Voudouris, P., Bieniok, A., Musso, M., and Amthauer G. (2009) A multi-analytical study of the crystal structure of unusual Ti–Zr–Cr-rich Andradite from the Maronia skarn, Rhodope massif, western Thrace, Greece. Mineralogy and Petrology, 95, 113–124.

Khoury, H.N. (2020) Geochemistry of rare earth elements (REE) and redox sensitive elements (RSE) of pyrometamorphic rocks, central Jordan. Arabian Journal of Geosciences, 13, 174.

Khoury, H., Salameh, E., and Clark I. (2014) Mineralogy and origin of surficial uranium deposits hosted in travertine and calcrete from central Jordan. Applied Geochemistry, 43, 49–65.

Khoury, H.N., Sokol, E.V, and Clark, I.D. (2015) Calcium uranium oxide minerals from central Jordan: assemblages, chemistry, and alteration products. The Canadian Mineralogist, 53, 61-82.

Khoury, H.N., Sokol, E.V., Kokh, S.N., Seryotkin, Y.V., Nigmatulina, E.N., Goryainov, S.V., Belogub, E.V., and Clark I.D. (2016) Tululite, $Ca_{14}(Fe^{3+},Al)(Al,Zn,Fe^{3+},Si,P,Mn,Mg)_{15}O_{36}$: a new Ca zincate-aluminate from combustion metamorphic marbles, central Jordan. Mineralogy and Petrology, 110, 125–140.

Kolodny, Y. (1979) Natural Cement Factory - A Geological Story. In: “Physics and Chemistry of Cement”, ed. J. Skalny, Plenum Press, N.Y., 203-216.

Kostić, S., Lazarević, Z.Ž., Radojević, V., Milutinović, A., Romčević, M., Romčević, N.Ž., and Valčić, A. (2015) Study of structural and optical properties of YAG and Nd:YAG single crystals. Materials Research Bulletin, 63, 80–87.

Kraus, W. and Nolze, G. (1996) POWDER CELL–a program for the representation and manipulation of crystal structures and calculation of the resulting X-ray powder patterns. Journal of Applied Crystallography, 29(3), pp.301-303.

Krot, A.N., Ma, C., Nagashima K., Davis, A.M., Beckett, J.R., Simon, S.B., Komatsu, M., Fagan, T.J., Brenker, F., Ivanova, M.A., and Bischoff, A. (2019) Mineralogy, petrography, and oxygen isotopic compositions of ultrarefractory inclusions from carbonaceous chondrites. Geochemistry, 79 (2019), 125519.

Lanzirotti, A. (1995) Yttrium zoning in metamorphic garnets. Geochimica et Cosmoschimica Acta, 59, 4105-4110.

Li, Z., Lee, W.D., and Zhang, S. (2007) Low-temperature synthesis of $CaZrO_3$ powder from molten salts. Journal of American Ceramic Society, 90, 364–368.

Ma, C. (2012) Discovery of meteoritic eringaite, $Ca_3(Sc,Y,Ti)_2Si_3O_{12}$, the first solar garnet? In: Conference materials of the 75th Annual Meteoritical Society Meeting 2012, 5015.

Ma, C., Yoshizaki, T., Krot, A.N., Beckett, J.R., Nakamura, T., Nagashima, K., Muto, J., and Ivanova M.A. (2017) Discovery of rubinite, $Ca_3Ti^{3+}{}_2Si_3O_{12}$, a new garnet mineral in refractory inclusions from carbonaceous chondrites. In: Conference materials of the 80th Annual Meeting of the Meteoritical Society 2017 (LPI Contrib. No. 1987), 6023.

Monteseguro, V., Rodríguez-Hernández, P., Vilaplana, R., Manjón, F. ., Venkatramu, V., Errandonea, D., Lavín, V., and Muñoz, A. (2014) Lattice dynamics study of nanocrystalline yttrium gallium garnet at high pressure. The Journal of Physical Chemistry C, 118, 13177−13185.

Novikov, I., Vapnik, Ye., Safonova, I. (2013) Mud volcano origin of the Mottled Zone, South Levant. Geoscience Frontiers, 4, 597-619.

Park, J.H. (2007) Formation of $CaZrO_3$ at the interface between CaO-SiO_2-MgO-CaF_2(-ZrO_2) slags and magnesia refractories: Computational and experimental study. Computer Coupling of Phase Diagrams and Thermochemistry (CALPHAD), 31, 149–154.

Picard, L. Geological research in the Judean Desert. Jerusalem, Goldberg Press, 1931. 108 p.

Pyle, J.M. and Spear, F.S. (1999) Yttrium zoning in garnet: Coupling of major and accessory phases during. Geological Materials Research, 1 (6), 49 pp.

Qu, M., Zhang, X., Mi, X., Liu, Q., and Bai, Z. (2020) Novel color tunable garnet phosphor of Tb^{3+} and Eu^{3+} co-doped $Ca_2YZr_2Al_3O_{12}$ with high thermal stability via energy transfer. Journal of Alloys and Compounds, 828, 154398.

Shannon, R.D. (1976) Revised effective ionic radii and systematic studies of interatomic distances in halides and chalcogenides. Acta Crystallographica, A32, 751–767.

Sharygin V.V. (2019) Orthorhombic $CaCr_2O_4$ in phosphide-bearing gehlenite-rankinite paralava from Hatrurim Basin, Israel: preliminary data. Conference: Magmatism of the Earth and Related Strategic Metal Deposits - 2019, p. 272-276. Saint Petersburg, Russia.

Schingaro, E., Scordari, F., Capitano, F., Parodi, G., Smith, D.C. and Motana, A. (2001) Crystal chemistry of kimzeyite from Anguillara, Mts. Sabatini, Italy. European Journal of Mineralogy, 13, 749-759.

Sokol, E.V., Kokh, S.N., Khoury, H.N., Seryotkin, Y.V., and Goryainov, S.V. (2016) Long-term immobilisation of Cd^{2+} at the Tulul Al Hammam natural analogue site, central Jordan. Applied Geochemistry, 70, 43-60.

Sokol, E.V., Kozmenko, O.A., Khoury, H.N., Kokh, S.N., Novikova, S.A., Nefedov, A.A., Sokol, I.A., and Zaikin P. (2017) Calcareous sediments of the Muwaqqar Chalk Marl

549 Formation, Jordan: Mineralogical and geochemical evidences for Zn and Cd enrichment.
550 Gondwana Research, 46, 204–226.

551 Sokol, E.V., Seryotkin, Y.V., Kokh, S.N., Vapnik, Ye., Nigmatulina, E.N., Goryainov,
552 S.V., Belogub, E.V., and Sharygin, V.V. (2015) Flamite, $(Ca,Na,K)_2(Si,P)O_4$, a new mineral
553 from ultrahigh-temperature combustion metamorphic rocks, Hatrurim Basin, Negev Desert,
554 Israel. Mineralogical Magazine, 79, 583-596.

555 Sokol, E.V., Kokh, S.N., Sharygin, V.V., Danilovsky, V.A., Seryotkin, Y.V., Liferovich,
556 R., Deviatiiarova, A.S., Nigmatulina, E.N., and Karmanov, N.S. (2019) Mineralogical
557 Diversity of Ca_2SiO_4-Bearing Combustion Metamorphic Rocks in the Hatrurim Basin:
558 Implications for Storage and Partitioning of Elements in Oil Shale Clinkering. Minerals, 9,
559 465.

560 Strocka, B., Holst, P., and Tolksdorf, W. (1978) An empirical formula for the calculation
561 of lattice constants of oxides garnets based on substituted yttrium- and gadolinium-iron
562 garnets. Philips Journal of Research, 33, 186–202.

563 Techer, I., Khoury, H.N., Salameh, E., Rassineux, F., Claude, C., Clauer, N., Pagel, M.,
564 Lancelot, J., Hamelin, B., and Jacquot, E. (2006) Propagation of high-alkaline fluids in an
565 argillaceous formation: Case study of the Khushaym Matruk natural analogue (Central
566 Jordan). Journal of Geochemical Exploration, 90, 53–67.

567 Thakur, S.S., Madhavan, K., Patel, S.C., Rameshwar, Rao D., Singh, A.K., Pandey, S.,
568 and Nandini, P. (2018) Yttrium-zoning in garnet and stability of allanite in metapelites from
569 the Main Central Thrust Zone and adjacent higher Himalayan Crystallines along the
570 Alaknanda Valley, NW Himalaya. Lithos, doi:10.1016/j.lithos.2018.09.002

571 Uher, P., Milovská, S., Milovský, R., Kodera, P., Bačík, P., and Bilohuščin, V. (2015)
572 Kerimasite, $\{Ca_3\}[Zr_2](SiFe^{3+}_2)O_{12}$ garnet from the Vysoká -Zlatno skarn, Štiavnica
573 stratovolcano, Slovakia. Mineralogical Magazine, 79(3), pp. 715–733.

Vaggelli, G., Borghi, A., Cossio, R., Mazzoli, C., and Olmi, F. (2003) Comparison between major and trace element concentrations in garnet performed by EPMA and micro-PIXE techniques. Spectrochimica Acta Part B, 58, 699–709.

Wang, X. and Wang, Yu. (2015) Synthesis, structure, and photoluminescence properties of Ce^{3+}-doped $Ca_2YZr_2Al_3O_{12}$: a novel garnet phosphor for white LEDs. The Journal of Physical Chemistry C, 119, 28, 16208–16214.

Wang, Yi., Ding, J., and Wang, Yu. (2017) $Ca_{2-x}Y_{1+x}Zr_{2-x}Al^{3+}_xO_{12}:Ce^{3+}$: Solid solution design toward the green emission garnet structure phosphor for near-UV LEDs and their luminescence properties. The Journal of Physical Chemistry C, 121, 48, 27018–27028.

Wang, X., Zhao, Z., Wu, Q., Li, Y., and Wang, Yu. (2016) A garnet-based $Ca_2YZr_2Al_3O_{12}:Eu^{3+}$ red-emitting phosphor for n‑UV light emitting diodes and field emission displays: electronic structure and luminescence properties. The Journal of Physical Chemistry C, 55, 21, 11072–11077.

Wright, K.I., Critchley, P., Garrard, A., Baird, D., Bains, R. and Groom, S. (2008) Stone Bead Technologies and Early Craft Specialization: Insights from Two Neolithic Sites in Eastern Jordan, Levant, 40:2, 131-165

Yeo, J.-G., Choi, S.-Ch., Kim, J.-W., Lee, J.-E., Lee, J.-H., and Jung, Y.-G. (2004) Thermal reaction behavior of $ZrSiO_4$ and $CaCO_3$ mixtures for high-temperature refractory application. Materials Science and Engineering, A368, 94–102.

Figure captions

Fig. 1. (A) Overall view of varicolored, layered pyrometamorphic marble. Priscillagrewite-(Y) occurs in the green layer, which is enriched in fluorapatite with vanadium impurity and low content of ellestadite end-member. In light-brown zones calcite is a major mineral, spurrite and fluorapatite with significant fluorellestadite end-member component are minor minerals. (B) BSE image of the green layer, which is largely fluorapatite (Ap) with calcite aggregates (Cal). Priscillagrewite-(Y) crystals are distributed sparsely in the fluorapatite. (C) BSE and optical image (in inset, transmitted light, PPL) of the priscillagrewite-(Y) crystal in Figure 1B, which was used for EBSD (see Fig. 3A-B). (D, E, F) BSE images of 3 other priscillagrewite-(Y) crystals; the crystal shown in Fig. 1D was studied using EBSD (see Fig. 3C-D).

Fig. 2. Raman spectrum of priscillagrewite-(Y) (blue) and surrounding its fluorapatie (red).

Fig. 3. EBSD patterns performed with garnet crystals shown in Fig. 1C, D and fitting results to the garnet structure with a = 12.50 Å.

Fig. 4. Crystal structure of priscillagrewite-(Y). Calcium at the dodecahedral *X* site is one-third replaced by Y+REE (blue - grey balls). The octahedral *Y* site is largely occupied by Zr (blue octahedra). The tetrahedral *Z* site contains Al > Fe^{3+} (green tetrahedra). Drawn with VESTA.

Fig. 5. A. *Y*-site diagram for discriminating mineral species in the bitikleite and schorlomite groups. Colored circles are corresponded to the holotype composition of minerals of the bitikleite group, the name of which is written the same color. B. *Z*-site diagram for discriminating bitikleite group garnets from schorlomite group garnets.

Fig. 6. Binary diagram 3Ca pfu – 3(Y+REE) pfu for occupancy of the *X* site with the compositional range of priscillagrewite-(Y) indicated by a red line and composition of the priscillagrewite-(Y) holotype specimen, by a pink circle. Generalized formulas of the Ca-garnet (bitikleite and schorlomite groups) and synthetic Y-garnet end-members are shown, together with the intermediate compositions (50/50). The inset shows the position of the binary system in the ternary Ca-Y+REE-Fe^{2+},Mn^{2+},Mg system for *X*-site occupancy.

Table 1. Chemical composition of priscillagrewite-(Y).

	wt%	s.d.	range	apfu
UO_3	0.58	0.32	0.21-1.02	0.01
Sb_2O_5	1.60	0.23	1.27-1.84	0.07
P_2O_5	0.44	0.19	0.13-0.61	0.04
HfO_2	0.09	0.03	0.06-0.14	0.00
ZrO_2	33.00	0.59	32.03-33.55	1.79
TiO_2	1.60	0.27	1.18-1.89	0.13
SiO_2	0.38	0.23	0.23-0.77	0.04
Al_2O_3	13.02	0.23	12.76-13.27	1.70
Fe_2O_3	14.42	0.29	14.00-14.77	1.21
CaO	18.40	0.26	18.28-18.90	2.19
Y_2O_3	11.02	0.63	10.33-11.73	0.65
La_2O_3	0.26	0.03	0.23-0.30	0.01
Ce_2O_3	0.87	0.16	0.61-1.06	0.03
Nd_2O_3	0.78	0.05	0.70-0.83	0.03
Sm_2O_3	0.17	0.07	0-0.27	0.01
Gd_2O_3	0.44	0.03	0.45-0.54	0.02
Dy_2O_3	0.67	0.04	0.63-0.74	0.02
Er_2O_3	0.61	0.04	0.58-0.67	0.02
Yb_2O_3	0.53	0.03	0.49-0.57	0.02
Total	98.88			

The empirical priscillagrewite-(Y) formula calculated on the basis of 12 O is $(Ca_{2.19}Y_{0.65}Ce^{3+}_{0.03}Nd^{3+}_{0.03}Gd^{3+}_{0.02}Dy^{3+}_{0.02}Er^{3+}_{0.02}Yb^{3+}_{0.02}La^{3+}_{0.01}Sm^{3+}_{0.01})_{\Sigma 3.00}(Zr_{1.79}Ti^{4+}_{0.13}Sb^{5+}_{0.07}U^{6+}_{0.01})_{\Sigma 2.00}(Al_{1.70}Fe^{3+}_{1.21}Si_{0.04}P^{5+}_{0.04})_{\Sigma 2.99}O_{12}$, which can be simplified to the formula $\{Ca_{2.19}(Y,REE)_{0.81}\}_{\Sigma 3.00}[(Zr,Ti)_{1.92}Sb^{5+}_{0.07}U^{6+}_{0.01}]_{\Sigma 2.00}([Al,Fe]_{2.91}Si_{0.04}P^{5+}_{0.04}]_{\Sigma 2.99}O_{12}$.

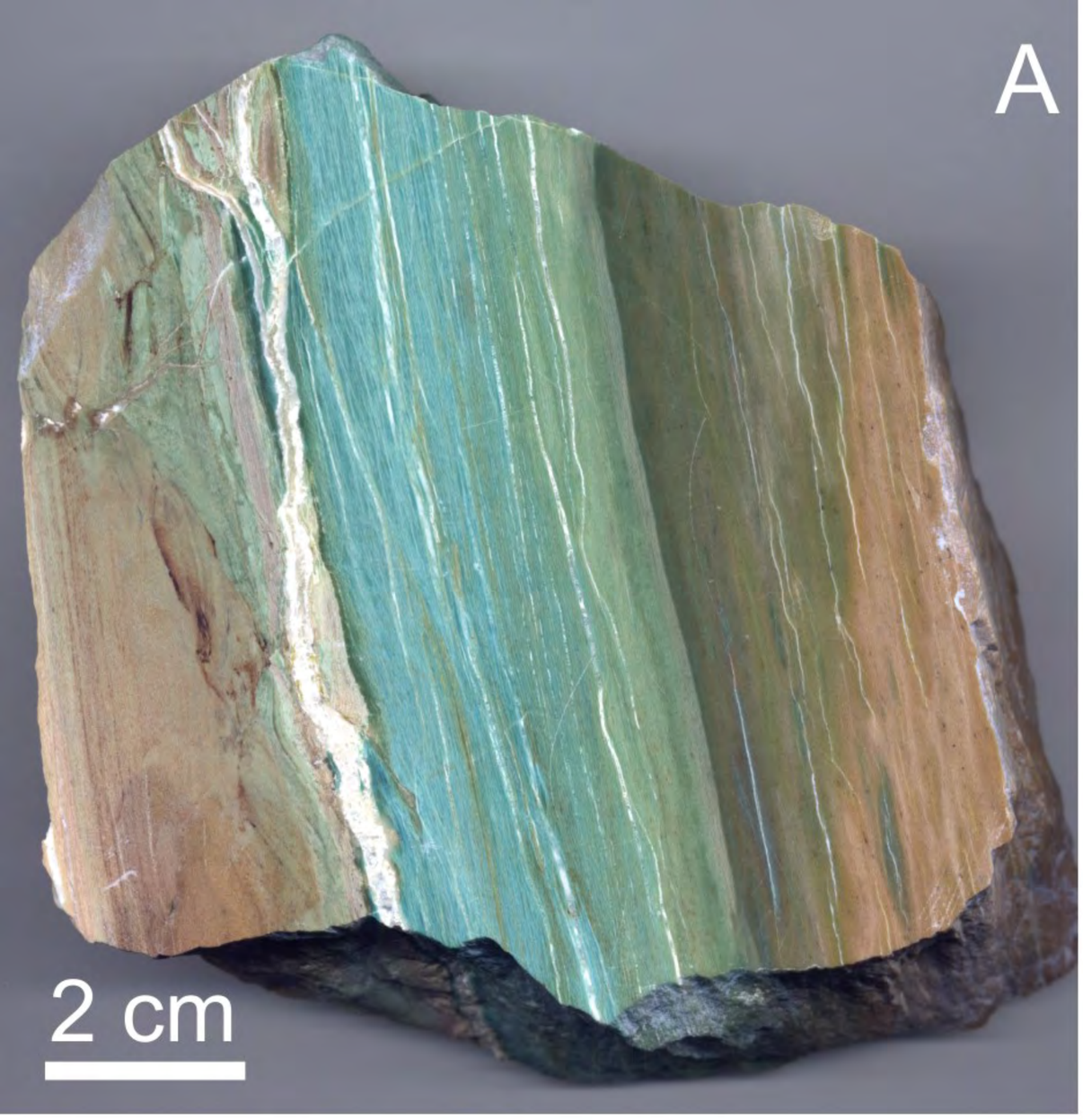

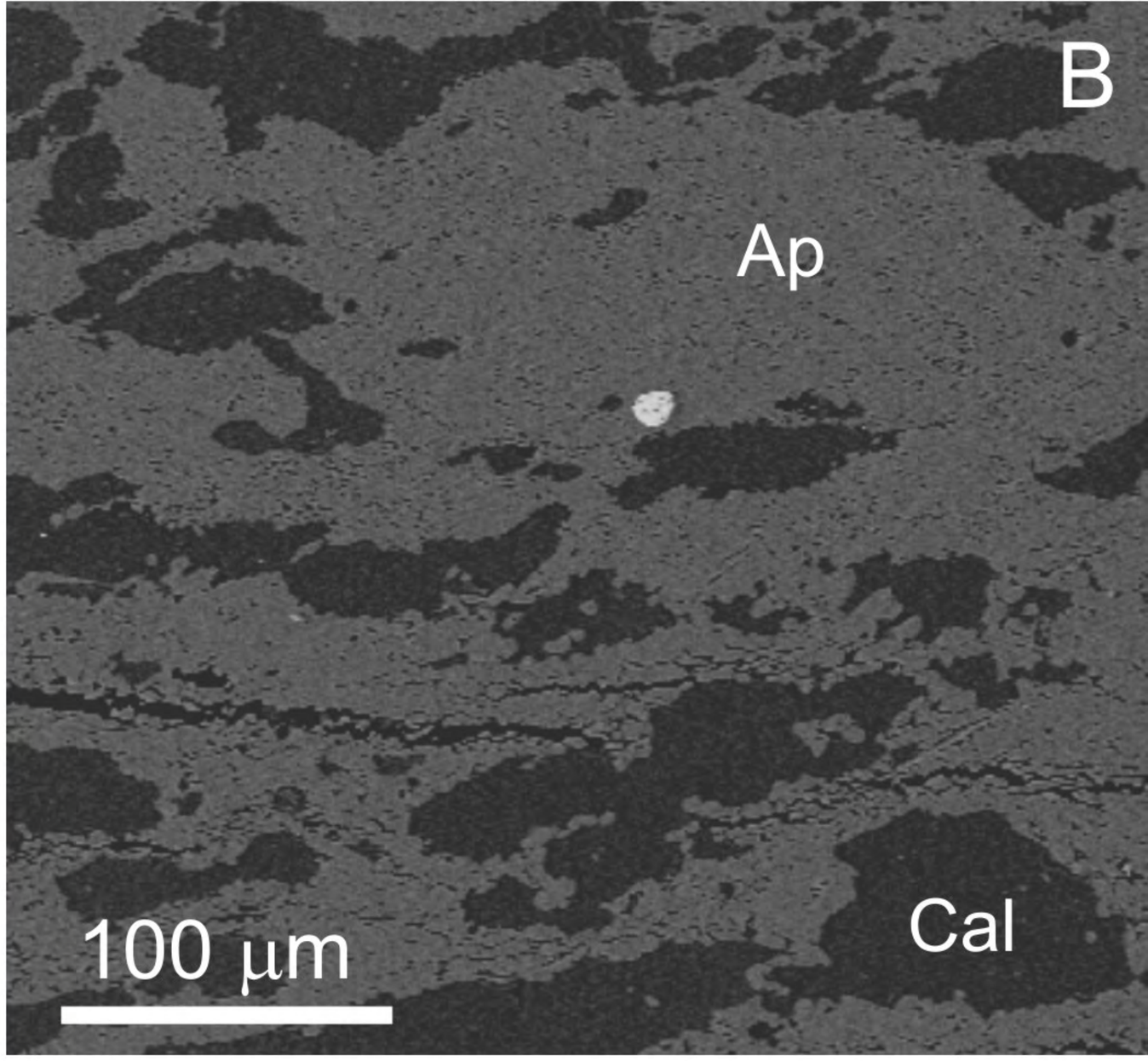

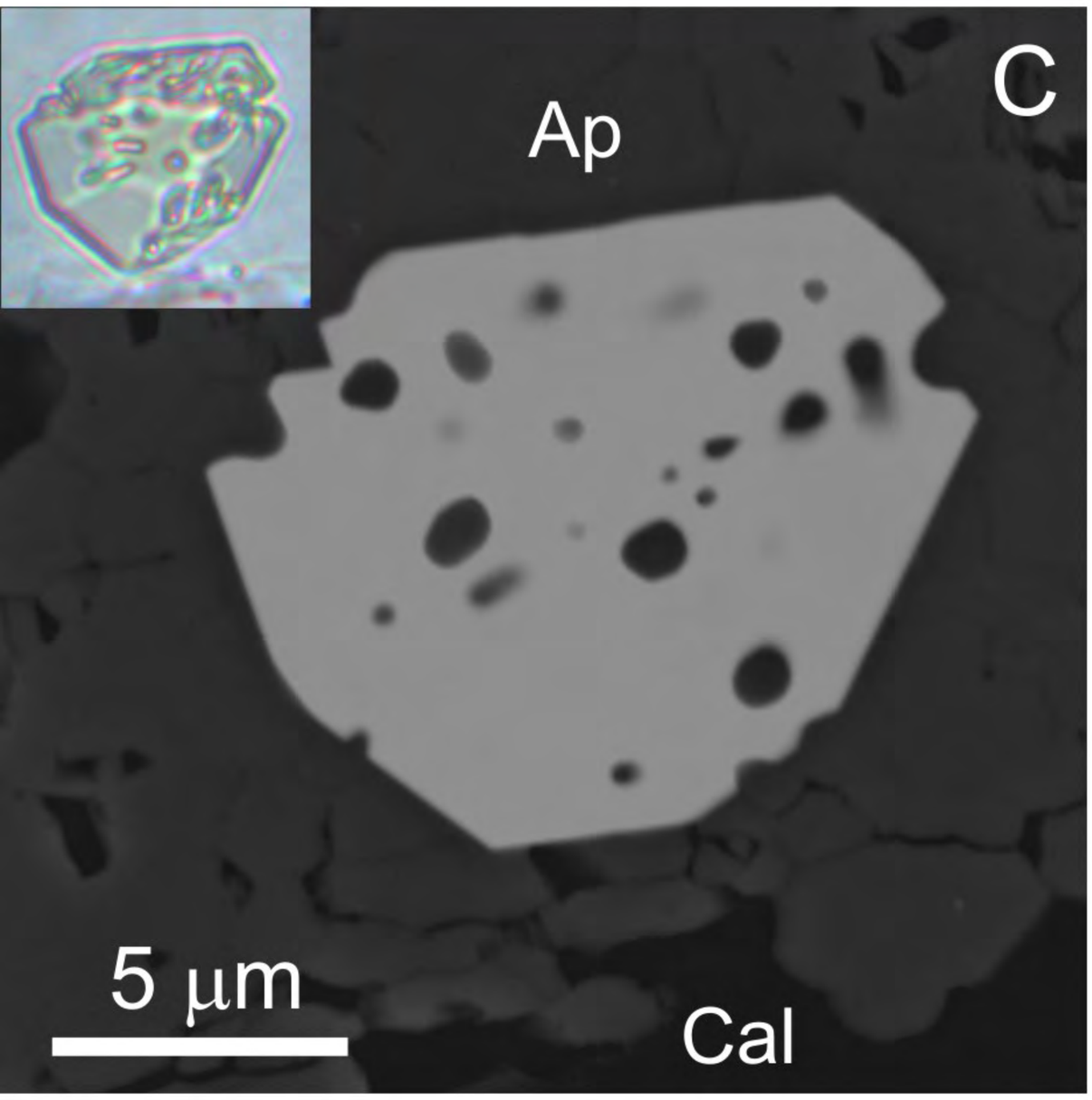

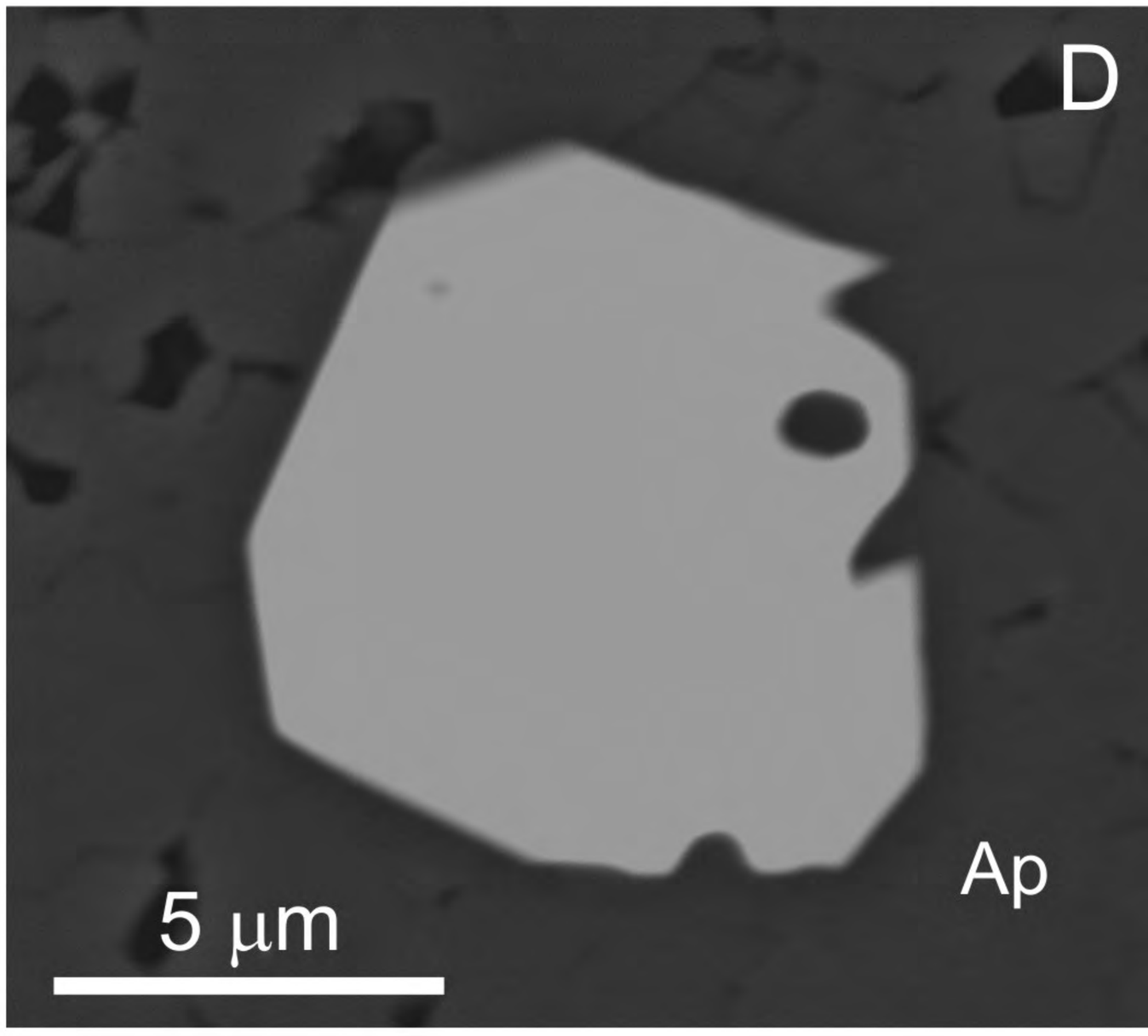

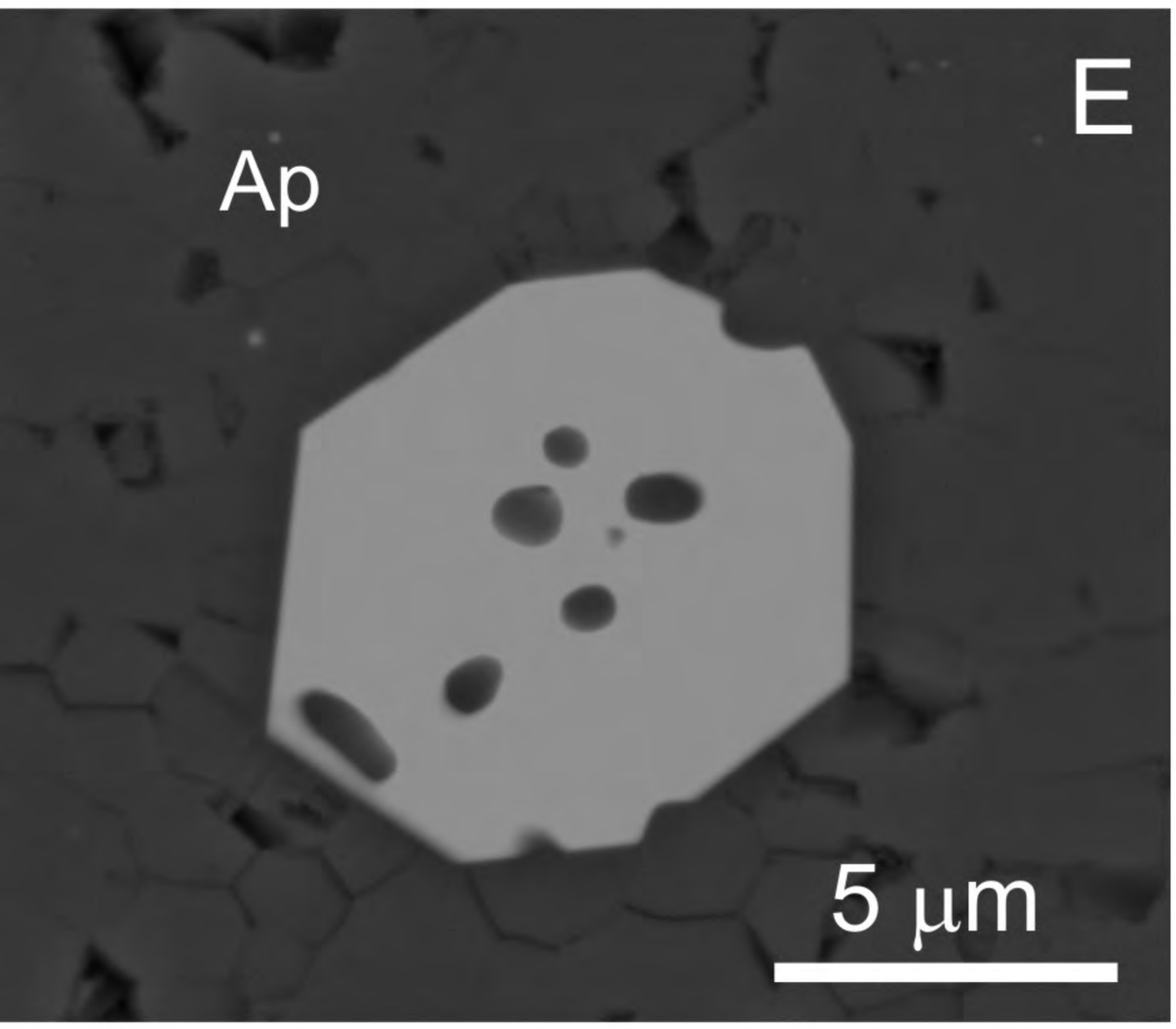

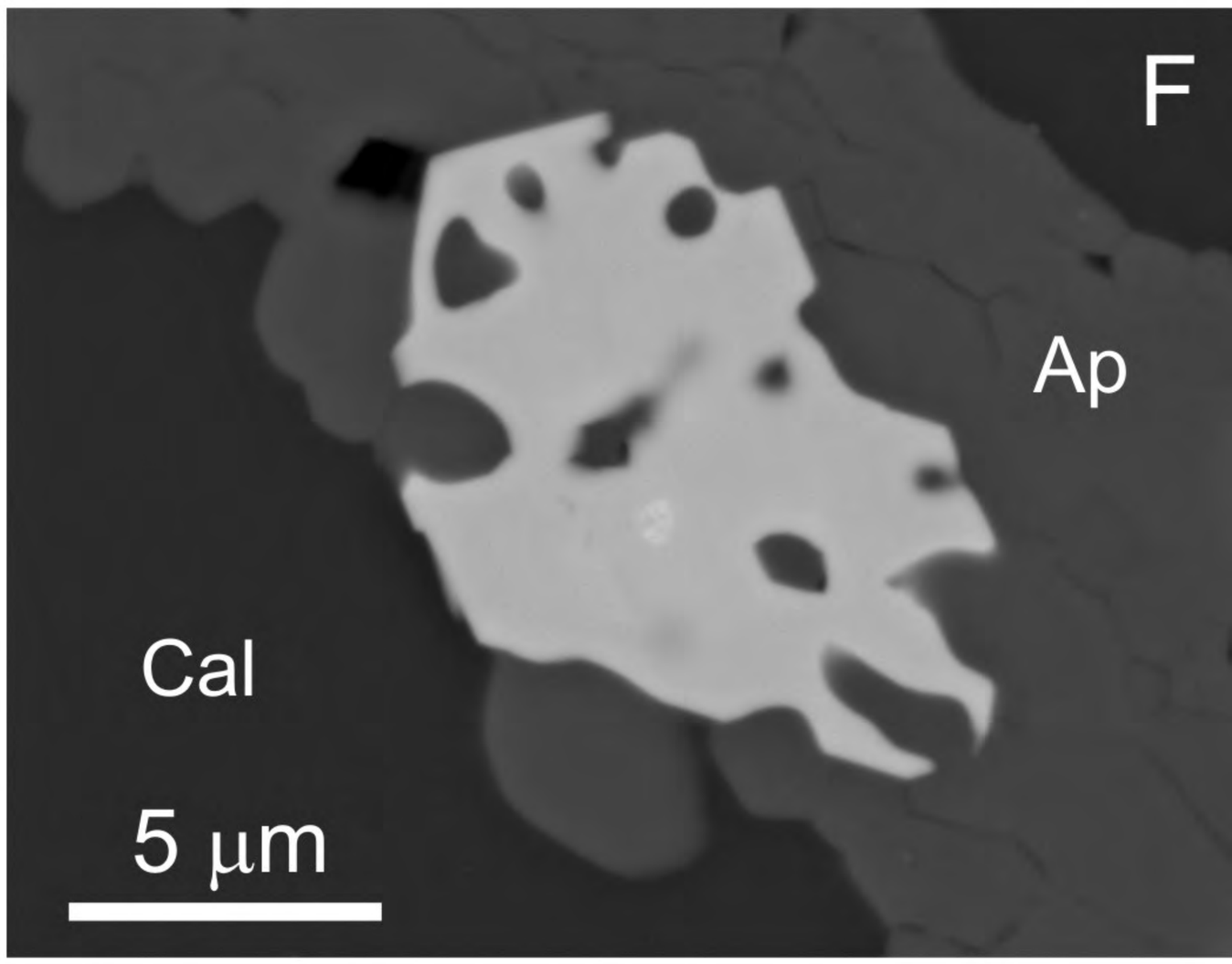

Fig. 1

Intensity [a.u.]

964
820
785
726
582
508
496
414
372
328
308
289
269
240
163
150

1200
1000
800
600
400
200

Raman shift (cm^{-1})

Fig. 2

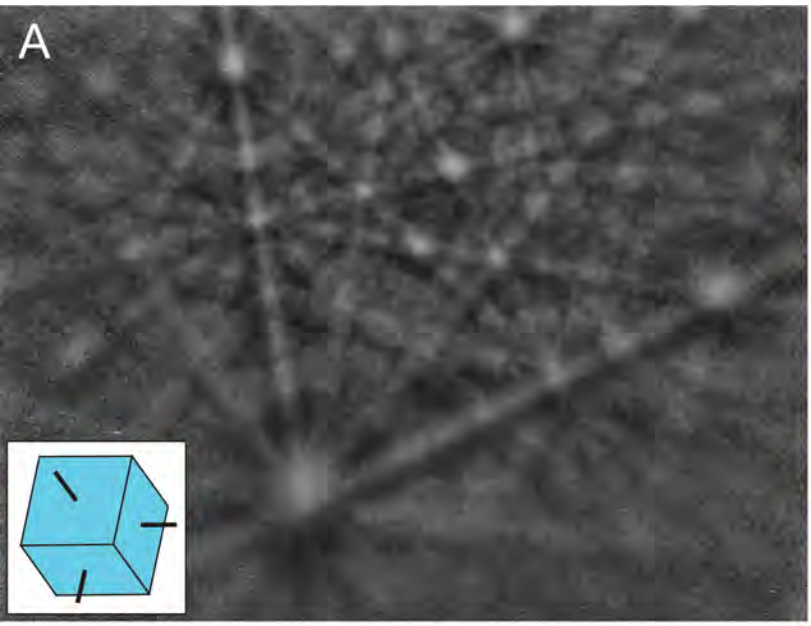
A

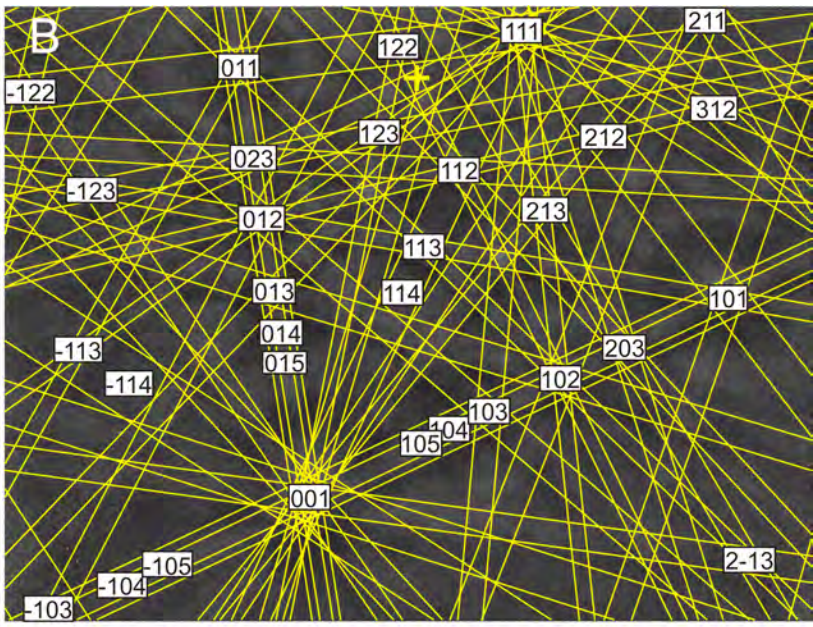
B
111
211
122
011
-122
312
123
212
023
112
-123
213
012
113
013
114
101
014
203
-113
015
102
-114
103
104
105
001
-105
2-13
-104
-103

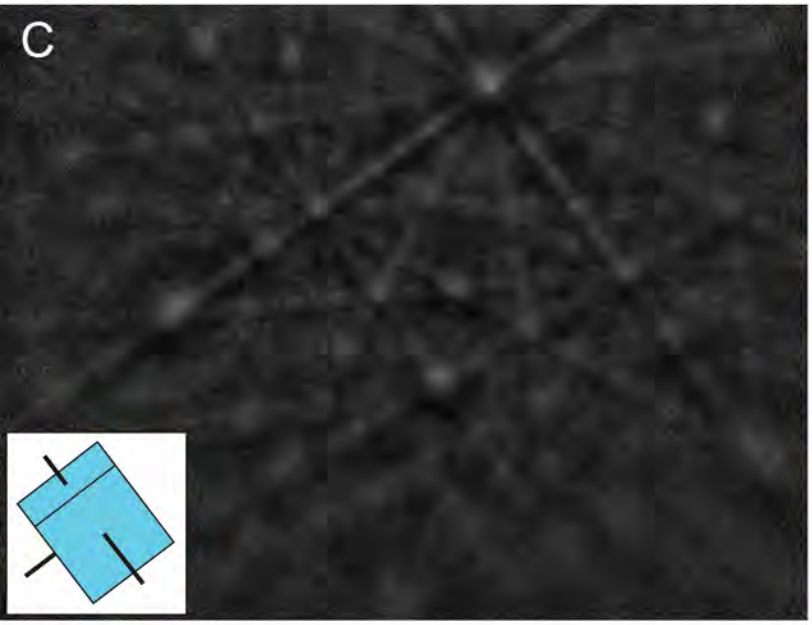
C

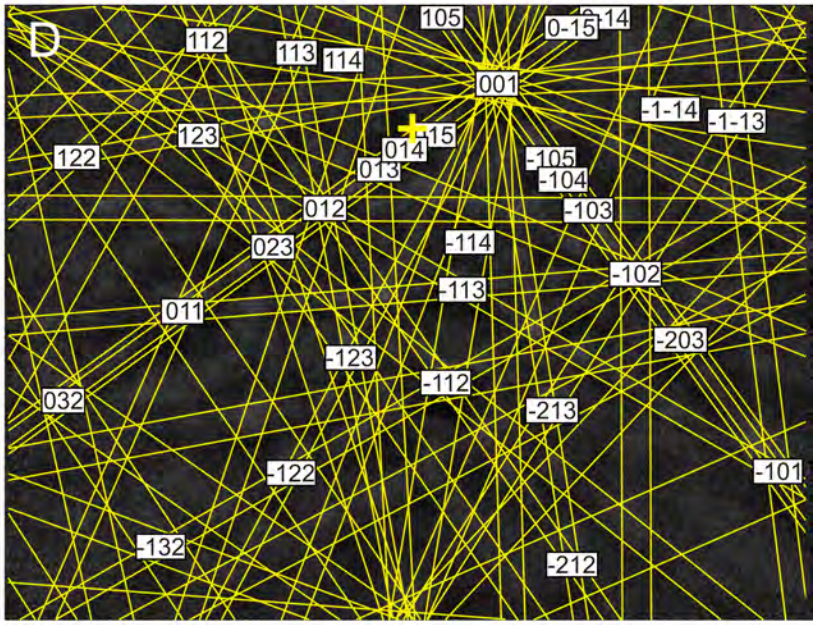
D
105
0-15
14
112
113
114
001
-1-14
-1-13
123
015
014
122
-105
013
-104
012
-103
023
-114
-102
-113
011
-203
-123
-112
032
-213
-122
-101
-132
-212

Fig. 3

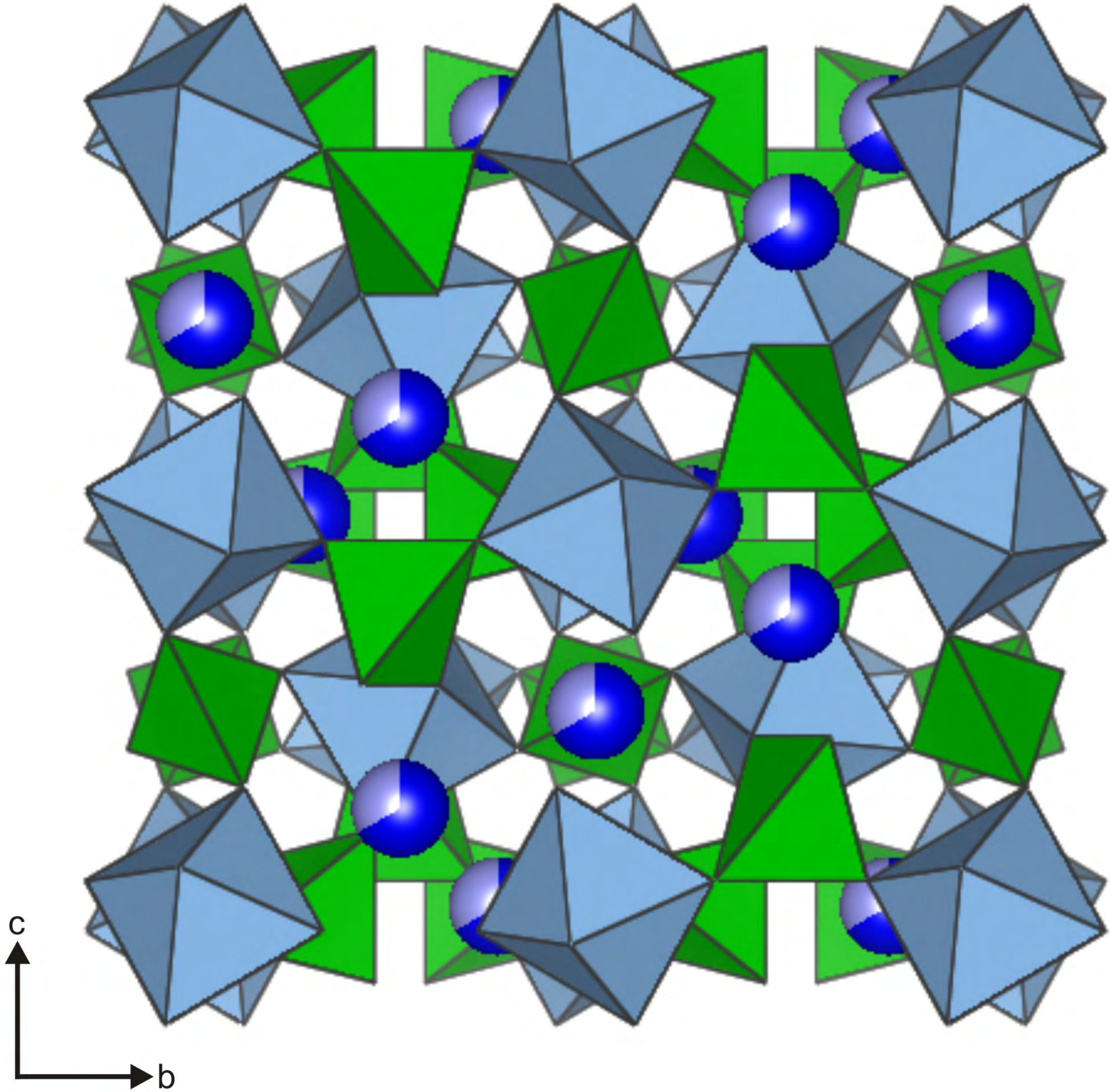

Fig. 4

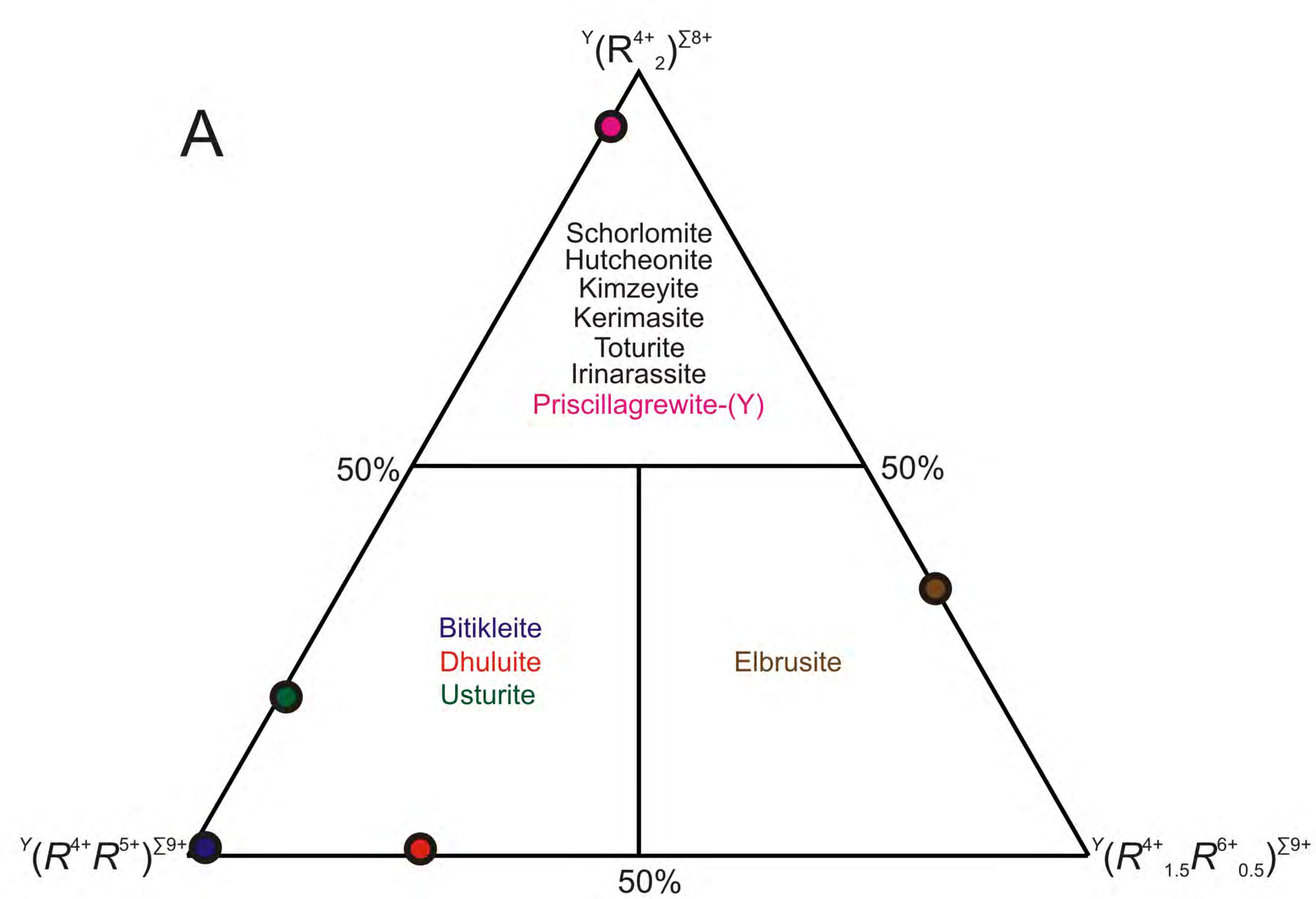
A
$^{Y}(R^{4+}_{2})^{\Sigma 8+}$
Schorlomite
Hutcheonite
Kimzeyite
Kerimasite
Toturite
Irinarassite
Priscillagrewite-(Y)
50%
50%
Bitikleite
Dhuluite
Usturite
Elbrusite
$^{Y}(R^{4+}R^{5+})^{\Sigma 9+}$
50%
$^{Y}(R^{4+}_{1.5}R^{6+}_{0.5})^{\Sigma 9+}$

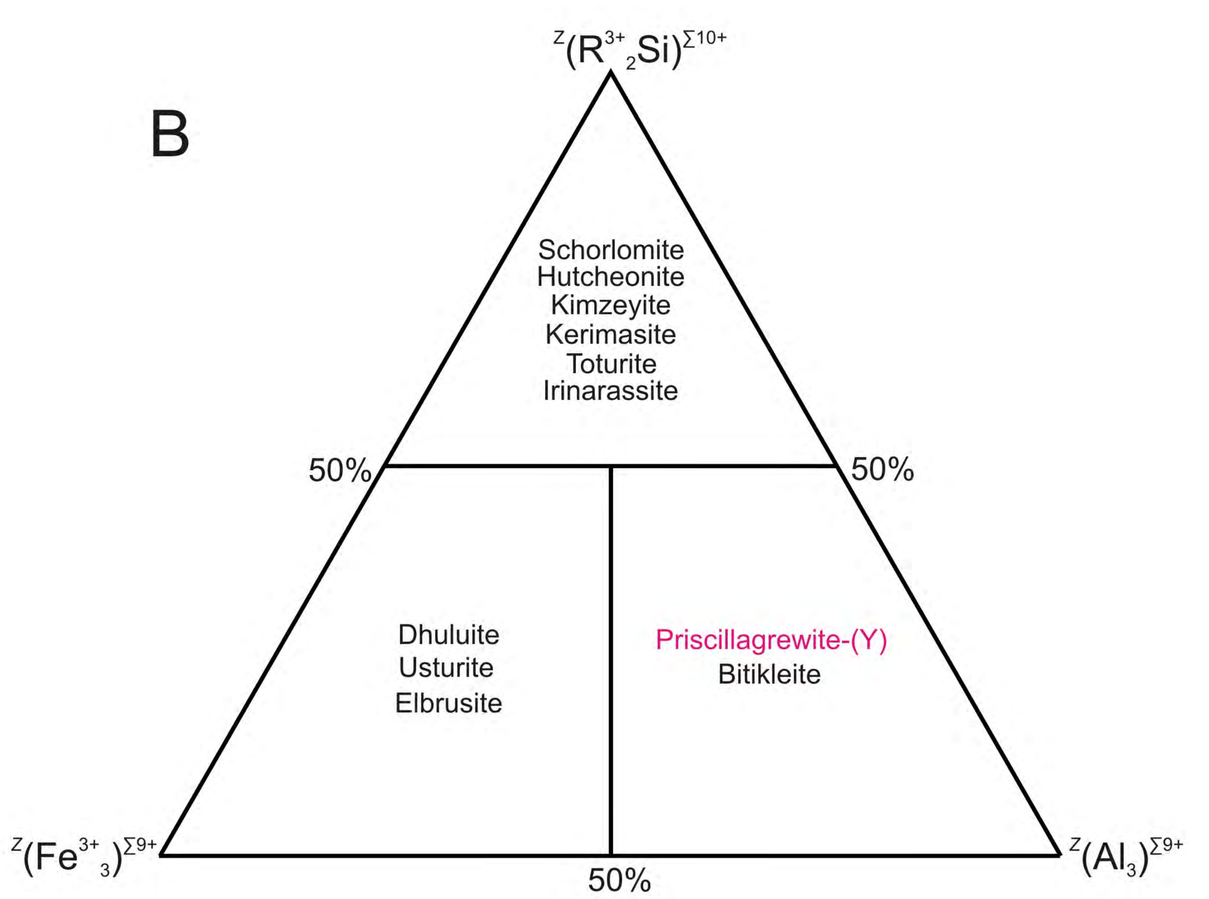
B
$^{Z}(R^{3+}_{2}Si)^{\Sigma 10+}$
Schorlomite
Hutcheonite
Kimzeyite
Kerimasite
Toturite
Irinarassite
50%
50%
Dhuluite
Usturite
Elbrusite
Priscillagrewite-(Y)
Bitikleite
$^{Z}(Fe^{3+}_{3})^{\Sigma 9+}$
50%
$^{Z}(Al_{3})^{\Sigma 9+}$

Fig. 5

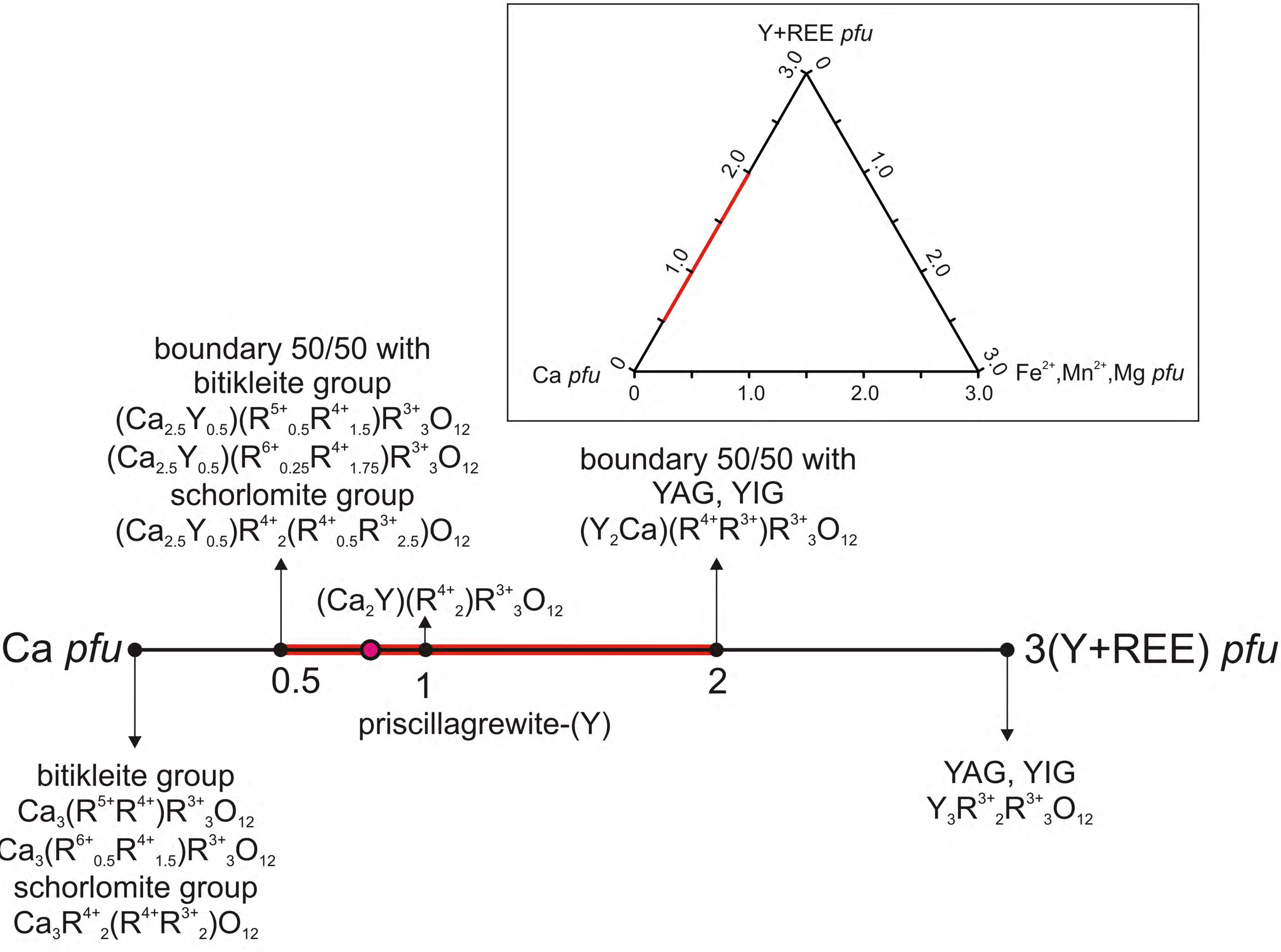
Y+REE *pfu*
3.0
0
2.0
1.0
1.0
2.0
3.0
Ca *pfu*
0
0
1.0
2.0
3.0
Fe^{2+},Mn^{2+},Mg *pfu*
boundary 50/50 with
bitikleite group
$(Ca_{2.5}Y_{0.5})(R^{5+}_{0.5}R^{4+}_{1.5})R^{3+}_{3}O_{12}$
$(Ca_{2.5}Y_{0.5})(R^{6+}_{0.25}R^{4+}_{1.75})R^{3+}_{3}O_{12}$
schorlomite group
$(Ca_{2.5}Y_{0.5})R^{4+}_{2}(R^{4+}_{0.5}R^{3+}_{2.5})O_{12}$
boundary 50/50 with
YAG, YIG
$(Y_2Ca)(R^{4+}R^{3+})R^{3+}_{3}O_{12}$
$(Ca_2Y)(R^{4+}_{2})R^{3+}_{3}O_{12}$
3Ca *pfu*
0.5
1
2
3(Y+REE) *pfu*
priscillagrewite-(Y)
bitikleite group
$Ca_3(R^{5+}R^{4+})R^{3+}_{3}O_{12}$
$Ca_3(R^{6+}_{0.5}R^{4+}_{1.5})R^{3+}_{3}O_{12}$
schorlomite group
$Ca_3R^{4+}_{2}(R^{4+}R^{3+}_{2})O_{12}$
YAG, YIG
$Y_3R^{3+}_{2}R^{3+}_{3}O_{12}$

Fig. 6